Accelerated Publications

Detection of an EPR Multiline Signal for the S_0* State in Photosystem II†

Johannes Messinger,‡ Jonathan H. A. Nugent,* and Michael C. W. Evans

Department of Biology, Darwin Building, University College London, Gower Street, London WC1E 6BT, U.K.

Received May 14, 1997; Revised Manuscript Received July 23, 1997⊗

ABSTRACT: The S_0* state was generated by incubation of dark-adapted (S_1 state) photosystem II membranes either with the exogenous two electron reductant hydrazine and subsequent 273 K illumination in the presence of DCMU or by dark incubation with low amounts of the one electron reductant hydroxylamine. In agreement with earlier reports, the S_1 and S_{-1} states were found to be electron paramagnetic resonance (EPR) silent. However, in the presence of 0.5−1.5% methanol, a weak EPR multiline signal centered around $g = 2.0$ was observed at 7 K for the S_0* states generated by both procedures. This signal has a similar average line splitting to the well-characterized S_2 state multiline EPR signal, but can be clearly distinguished from that and other modified S_2 multiline signals by differences in line position and intensities. In addition, at 4 K it can be seen that the S_0* multiline has a greater spectral breadth than the S_2 multilines and is composed of up to 26 peaks. The S_0* signal is not seen in the absence of methanol and is not affected by 1 mM EDTA in the buffer medium. We assign the S_0* multiline signal to the manganese cluster of the oxygen evolving complex in a mixed valence state of the form $Mn^{II}Mn^{III}Mn^{III}Mn^{III}$, Mn^{II}-$Mn^{III}Mn^{IV}Mn^{IV}$, or $Mn^{III}Mn^{III}Mn^{III}Mn^{IV}$. Addition of methanol may be helpful in future to find an EPR signal originating from the natural S_0 state.

Photosystem II (PS II)[1] is a membrane bound chlorophyll−protein complex that utilizes the energy of visible light to catalyze (a) the reduction of plastoquinone to plastohydroquinone and (b) the oxidation of water to molecular oxygen and protons. While each light-induced charge separation between the PS II reaction center chlorophyll P680 and a pheophytin molecule, Pheo, generates one oxidizing and one reducing equivalent, reaction a involves the cooperation of two electrons and reaction (b) requires the cooperation of four strongly oxidizing equivalents within the oxygen evolving complex (OEC). The oxidation of the OEC by $P680^{\bullet+}$ occurs via a redox active tyrosine residue, Y_Z, of the reaction center polypeptide D1 (for reviews, see refs 1−5).

During water oxidation, the OEC cycles through five different redox states termed S_0, S_1, ..., S_4 (*6*). After long dark adaptation practically all PS II centers are in the redox state S_1, because S_2 and S_3 are reduced to S_1 by electrons from the reduced forms of the primary and secondary quinone electron acceptors, Q_A^-, Q_B^-, and Q_B^{2-}, or from the redox active tyrosine Y_D of the reaction center polypeptide D2. In its oxidized form, Y_D^{ox} slowly converts S_0 into S_1 during dark adaptation (*7, 8*). The S_4 state of Kok's scheme is only transiently populated during oxygen formation in the $S_3 \rightarrow S_0$ transition and possibly reflects the state $S_3Y_Z^{ox}$.

A complex of four manganese ions probably organized in two pairs of μ-oxo-bridged dimers was found to be essential for the process of water oxidation and to store at least part of the four oxidizing equivalents (for review, see refs 1−5 and 9). While the dark stable S_1 state does not show an EPR signal, the S_2 state is paramagnetic and is detected as the so called "multiline" signal which is centered around $g = 2.0$ (*10*). The $S_1 \rightarrow S_2$ transition is thought to reflect a manganese oxidation. The S_2 state can be generated in high yield by continuous illumination at 200 K, or at 273 K in the presence of the herbicide, 3-(3,4-dichlorophenyl)-1,1-dimethylurea (DCMU). Both procedures restrict PS II to one stable charge separation, either by a thermal block of the reactions $S_2 \rightarrow S_3$ and $Q_A^-Q_B \rightarrow Q_AQ_B^-$ or by preventing the binding of Q_B. The S_2 multiline signal has been simulated and is believed to originate either from an isolated $Mn^{III}Mn^{IV}$ dimer with unusual ligand geometry (*11*) or from a $Mn^{III}Mn^{IV}$ dimer magnetically coupled to another dimer (*12*) in the redox states $Mn^{III}Mn^{III}$ (*13*) or $Mn^{IV}Mn^{IV}$ (*14*). The hyperfine splitting of the S_2 state multiline signal depends on many factors such as the cryoprotectant, the addition of alcohols, ammonia, and the depletion of Ca^{2+}

† The authors acknowledge financial support by the European Community through a Human Capital Mobility Grant and the Biotechnological and Biological Sciences Research Council.

* Author to whom correspondence should be addressed.

‡ Present address: Structural Biology Division, Lawrence Berkeley Laboratory, University of California, Berkeley, CA 94720.

⊗ Abstract published in *Advance ACS Abstracts,* August 15, 1997.

[1] Abbreviations: [Chl], chlorophyll concentration; cytb_{559}, cytochrome b_{559}; DCMU, 3-(3,4-dichlorophenyl)-1,1-dimethylurea, an inhibitor of electron transfer from Q_A to Q_B in PS II; EDTA, ethylenediaminetetraacetic acid, a chelator of bivalent metal ions (e.g., Mn^{2+}); EPR, electron paramagnetic resonance; OEC, oxygen evolving complex; PS II, photosystem II; P680/$P680^{\bullet+}$; primary electron donor in PS II and its cation radical form; Pheo, pheophytin, the electron acceptor during the primary charge separation in PS II; Q_A, plastoquinone of PS II that acts as a one electron acceptor to $Pheo^-$; Q_B, reversibly bound plastoquinone molecule that acts as a two electron acceptor to Q_A^-; S_i states, redox states of the OEC in PS II, *i* indicates the number of stored oxidizing equivalents relative to the lowest natural redox state (S_0); S_0* state, S_0 state produced by incubation of PS II preparations with exogenous reductants; Y_D, redox active tyrosine of the D2 polypeptide of PSII; Y_Z, redox active tyrosine of the D1 polypeptide of PS II that acts as the electron donor to $P680^{\bullet+}$ and in turn oxidizes the OEC.

S0006-2960(97)01128-8 CCC: $14.00

and therefore several different forms of the S_2 multiline exist (for review, see ref 1). Under certain conditions, such as the absence of alcohols in combination with cryoprotectants such as sucrose, the presence of certain inhibitors, e.g., fluoride and ammonia or illumination at 130 K, another S_2 state EPR signal around $g = 4.1$ is seen (see refs 1, 15, and 16 for review).

Several experiments, such as S_i state dependent shifts or changes of (a) X-ray absorption edge positions (*17*), (b) Y_D^{ox} spin lattice relaxation (T_1) times (*18*, *19*) or (c) electrochromic shifts and UV absorption spectra (for review, see ref 20), indicate strongly that the $S_0 \rightarrow S_1$ transition also involves a manganese oxidation and that consequently the manganese cluster in the S_0 state has two electrons more than in the S_2 state. Therefore, S_0 should be paramagnetic, and one expects to find an EPR signal. However, so far, no EPR signal has been reported in samples enriched in S_0 either by illumination of dark adapted samples (S_1) with three flashes or by incubation with exogenous reductants (*19*, *21*−*24*). One of the following factors may have prevented the discovery of an S_0 state EPR signal in previous studies: the S_0 state concentrations were not high enough, conditions were used where some S_2 was generated along with S_0, which may have masked a weaker S_0 EPR signal, the correct EPR conditions or combinations of cryoprotectants and additions were not used.

In this study, we exploit the known effects of hydrazine and hydroxylamine to generate samples enriched in S_0 with final chlorophyll (Chl) concentrations of greater than 10 mg/mL. To indicate the possibility that the electronic configuration of these chemically induced S_0 states might be different from that of the "natural" S_0 state in untreated samples, the notation S_0* was introduced earlier (*24*) and is also used here. Hydrazine and hydroxylamine were shown to reduce the manganese cluster of the OEC in the dark to S_i states below S_1, namely S_0, S_{-1}, S_{-2}, and S_{-3} (*25*−*29*). Recently, it was shown that hydrazine reacts as a two electron donor toward the OEC reducing S_1 directly into S_{-1} [a further reduction to the S_{-3} state proceeds with an about 50 times slower rate constant (*29*)], while hydroxylamine is a one electron donor (*30*). Therefore, two possibilities exist to generate S_0* populations with these reductants: (a) incubation with hydrazine to generate a high S_{-1} population which can then be converted into S_0* by illumination either at 200 K or at 273 K in the presence of DCMU. This procedure gives potentially a high S_0* population (*27*, *30*), but is coupled with some Mn^{2+} release from the OEC; (b) incubation with low concentrations of hydroxylamine (∼1 NH_2-OH per PS II reaction center). As the rate of S_0* reduction to S_{-1} is twice as fast as the S_1 reduction to S_0*, an S_0* population of about 30% can be achieved (*30*). This method does not involve any illumination and therefore the formation of S_2 state EPR signals is excluded.

A new EPR multiline signal was found with both procedures if 0.5−1.5% methanol was added to the samples. We therefore assign this new multiline signal to the S_0* state. Possible electronic configurations of the manganese ions in S_0* are discussed.

EXPERIMENTAL PROCEDURES

PS II membranes were prepared from market spinach under dim green light according to (*31*) with the following modifications: (a) all steps were carried out in a buffer medium containing 400 mM sucrose, 15 mM NaCl, 5 mM $MgCl_2$, and 50 mM Mes/NaOH, pH 6.3, (b) the chloroplast envelopes were broken using a homogenizer, (c) the Triton incubation was performed in the dark on ice for 20 min using 0.13 mL of 20% Triton solution (in buffer)/mg of Chl. The chlorophyll concentration, [Chl], was determined according to ref 32. After the final spin, the PS II membranes were resuspended in buffer to a [Chl] = 7−10 mg/mL and frozen as beads by slowly dropping the suspension into liquid nitrogen. The preparations were stored until used either in liquid N_2 or at −75 °C. No EDTA was added during the preparation procedure. Typical rates of oxygen evolution were 400−500 μmol of O_2/mg of Chl/h and the Chl a:Chl b ratio was in the range 2.1 −2.5:1.

EPR Spectrometry. EPR measurements at cryogenic temperatures were performed using a Jeol RE1X spectrometer fitted with an Oxford Instruments liquid helium cryostat. Spectra were recorded using a Dell microcomputer running Asyst software. Instrumental conditions are given in the figure legends. Some spectra had a linear background slope subtracted to improve presentation of figures. $P_{1/2}$, the microwave power at half saturation, was calculated by fitting a curve to a plot of signal amplitude versus square root of the microwave power.

Preparation of PS II Membrane Fragments Enriched in the S_0 State.* All procedures, with the exception of the 200 and 273 K illuminations, were performed in the dark or very dim green light.

Hydrazine Treatment. The PS II membrane fragments were thawed on ice and diluted to a [Chl] = 3.7 mg/mL with "mannitol buffer" of the following composition: 400 mM mannitol, 20 mM $CaCl_2$, 10 mM $MgCl_2$, and 50 mM Mes/NaOH, pH 6.3 (adjusted at 20 °C). Of this solution, 800 μL was then transferred into 2 mL Eppendorf tubes and kept on ice until used. Hydrazine was added from a 10 mM stock solution of $N_2H_6SO_4$ in mannitol buffer (adjusted to pH 6.5 at 20 °C) to give final hydrazine concentration of 2 mM and [Chl] = 3 mg/mL, respectively. The samples were incubated for 30 min on ice. DCMU was then added from a 25 mM methanolic stock solution to give a final DCMU concentration of 250 μM (final methanol concentration, 1%). After further 10 min incubation on ice, the reaction was slowed down by a 2-fold dilution with ice-cold mannitol buffer. The sample was then immediately centrifuged for 10 min at 11 000 rpm in a refrigerated Eppendorf centrifuge (model 5403). The spin conditions were optimized to give a soft pellet ([Chl] = 20−25 mg/mL) as harsher spin conditions increased the amount of Mn^{2+} release. The pellets were transferred into special plastic holders designed to permit loading of pellets for EPR and then either frozen immediately in liquid nitrogen (S_{-1} samples) or first illuminated at about 273 K for 1 min with an unfiltered 1000 W light source before freezing. Control samples were prepared in the same way except for the addition of hydrazine. Illumination at 200 K was carried out in an ethanol dry ice (solid CO_2) bath within an unsilvered glass Dewar. The samples were protected from the ethanol with small clear plastic tubes and illuminated for 6 min from both sides with the light source described above.

Hydroxylamine Treatment. Before the incubation, the PS II membranes were thawed in a water bath (20 °C) for about 20 min and then diluted 5−10-fold with cold mannitol buffer.

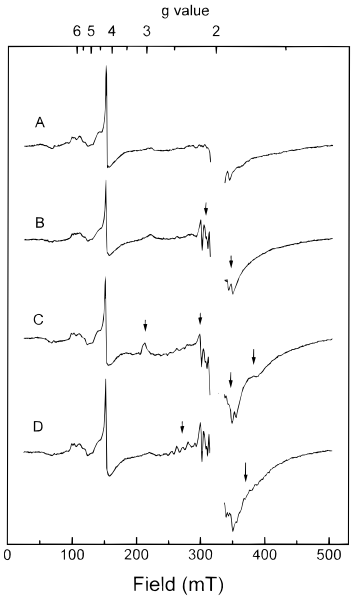

FIGURE 1: EPR spectra from PS II membrane pellets ([Chl] = 20−25 mg/mL) at 7 K: spectrum A, dark adapted control (S_1 state); spectrum B, after 40 min incubation with 2 mM hydrazine on ice at pH 6.5 and 10 min centrifugation (S_{-1} state); spectrum C, as in spectrum B, but after 200 K illumination; spectrum D, as in spectrum B, but after 273 K illumination in the presence of DCMU (S_0 state). Instrument conditions: microwave power, 10 mW; microwave frequency, 9.066 GHz; magnetic field modulation frequency, 100 kHz; magnetic field modulation amplitude, 1.6 mT; time constant, 0.1 s; scan time, 2 min. Each spectrum is the average of two scans.

The membranes were centrifuged at 2 °C for 20 min at 40000*g* and further dark adapted for 2 h. The pellet was resuspended in a small volume of mannitol buffer to a final [Chl] of about 14 mg/mL. Aliquots of 400 μL of the suspension were transferred into calibrated quartz EPR tubes with an inner diameter of 3 mm and kept on ice until used. Shortly before the start of the hydroxylamine treatment, 6 μL of methanol (final concentration 1.5%) and 4 μL of EDTA solution (100 mM stock, pH 6.5, final concentration 1 mM) were added if indicated in the figure legends. Hydroxylamine was added from a freshly prepared and pH adjusted $NH_2OH{\cdot}HCl$ stock solution (5 mM, pH 6.3−6.5, 20 °C) in mannitol buffer to a final concentration of 50 μM (~1 molecule NH_2OH per PS II complex, assuming 250 Chl per reaction center) and incubated for 10 min on ice. The reaction was terminated by freezing the tube in liquid N_2.

Mn Determination. The percentage of Mn released from PS II membranes during incubation with hydrazine or hydroxylamine was determined in the absence of EDTA by measuring the six-line Mn^{2+} EPR signal. Samples or aliquots taken at various steps during the treatments were compared to the size of the signal that can be generated in a control of the same [Chl] by a 10 min dark incubation in a water bath of 50−60 °C. The EPR measurements of the Mn^{2+} signals were performed under the following conditions: temperature, 11 K; microwave power, 0.01 and 1 mW; magnetic field modulation amplitude, 1 mT.

RESULTS

In Figure 1A an EPR trace of dark adapted PS II membranes is displayed, which was obtained from a pellet with a [Chl] = 20−25 mg/mL. It shows the typical signals for (a) rhombic iron at $g = 4.3$, (b) high spin iron at $g = 6$ from the cytochrome *b*/*f* complex, and (c) Rieske iron-sulfur center at $g = 1.9$. Except for very small signals at $g_z = 2.9$ and $g_y = 2.2$ from some oxidized low potential cytb_{559}, no signals related to PS II cofactors are present. The region around $g = 2.0$ containing the large signal from tyrosine Y_D^{ox} has been deleted. The spectrum in Figure 1B was obtained after a 40 min incubation of PS II membranes on ice with 2 mM hydrazine at pH 6.5. From the oxygen oscillation pattern measured under similar conditions (*30*) it is known that this treatment leads to a reduction of the S_1 state into the S_{-1} state. No signals attributed to the formation of the S_{-1} state are detected. From the appearance of the typical hexaquo Mn^{2+} signal (arrows), it is clear that some PSII centers have lost their manganese. The Mn^{2+} signal in Figure 1B represents about 12% of the manganese left in the pellet (data not shown). A comparison of the size of the Mn^{2+} signal with those that can be generated in a control and in the S_{-1} sample by heat treatment shows that the hydrazine incubation leads to a conversion of approximately 35% of manganese into Mn^{2+}, of which a part remains in the supernatant after centrifugation.

In control samples (S_1 state), 200 K illumination leads to an almost complete transition of the sample into the $S_2Q_A^-$ state and to the formation of the S_2 multiline signal around $g = 2.0$ (*10*). Therefore, a small remaining population of S_1 in the S_{-1} sample would result in the formation of some S_2 state multiline signal upon 200 K illumination. This was tested in Figure 1C. No multiline signal (or $g = 4.1$) is detected showing the complete conversion of the sample into states below S_1. In contrast to earlier reports (*22*−*24*), we find that 200 K illumination of our S_{-1} sample leads preferentially to the oxidation of the high potential cytb_{559} (peaks at $g_z = 3.08$ and $g_y = 2.15$, see arrows Figure 1C) rather than of the manganese cluster, as the size of the cytb_{559} signals correspond well to the amplitudes that can be induced by 77 K illumination of similar S_{-1} samples (data not shown). This observation, which could indicate a thermal block of the $S_{-1} \rightarrow S_0$* transition in our samples, was not further investigated in this study, but may be due to the use of different reductants (hydrazine versus hydroxylamine) or differences in the buffer compositions. The two arrows on the high-field side of $g = 2$ (Figure 1C) point to the signals arising from the $Q_A^-Fe^{2+}$ complex at the electron acceptor side of PS II. In order to circumvent a possible thermal block for the $S_{-1} \rightarrow S_0$* transition at 200 K, we also performed a continuous illumination at about 273 K in the presence of DCMU on another S_{-1} sample (Figure 1D). DCMU blocks the electron transport between Q_A and Q_B and therefore allows only a single turnover of the OEC. No oxidation of cytb_{559} is observed under these conditions, but the formation of a multiline signal centered around $g = 2.0$ does occur.

Figure 2 illustrates this finding in more detail, concentrating on the region around $g = 2.0$. Figure 2B shows a light minus dark difference spectrum of a control S_1 sample, where the S_2 multiline was generated by 273 K illumination in the presence of DCMU. Figure 2A shows the 200 K illuminated minus dark difference spectrum of an S_{-1} sample. This shows that no multiline signal is observed after 200 K illumination of the S_{-1} sample obtained after hydrazine treatment. The arrows indicate (a) the $g_y = 2.15$ signal of the oxidized high-potential cytb_{559} and b, c, and d the 1.9, 1.8, and 1.64 forms of the $Q_A^-Fe^{2+}$ signal, respectively. As this difference spectrum was obtained from a sample that

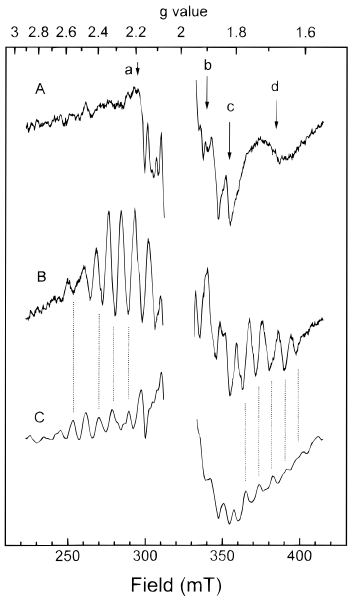

FIGURE 2: Illuminated minus dark EPR difference spectra of PSII membranes: spectrum A, 200 K illumination of S_{-1} sample in presence of DCMU; spectrum B, S_2 multiline induced by 273 K illumination of a control sample (S_1) in presence of DCMU; spectrum C, S_0* multiline signal induced by 273 K illumination of S_{-1} sample in presence of DCMU. The S_{-1} samples were generated by incubation with hydrazine as described in Figure 1 and in Experimental Procedures. Instrument conditions: As in Figure 1 but with a time constant of 0.3 s; scan time, 4 min. Spectra A and B are the average of two scans, while spectrum C is the average of eight scans.

does not contain EDTA, some small subtraction artifacts in the region of the six line Mn^{2+} signal are also visible. Figure 2C depicts the light minus dark difference spectrum obtained by 273 K illumination of a S_{-1} sample in the presence of DCMU. Under these conditions, the formation of a multiline signal takes place. A comparison of the two multiline signals shows that they are different in several peak positions and relative intensities (dotted lines).

The most straight forward interpretation of these results is to attribute the new multiline signal to the S_0* state that can be expected to be formed from the S_{-1} state under the conditions of Figure 2C. However, it is difficult to exclude the possibility that at 273 K illumination, an altered S_2 state multiline signal is formed from centers in a modified S_1 state. We therefore used the one electron reductant hydroxylamine to produce S_0* from dark-adapted samples without any illumination step.

At low hydroxylamine concentrations, a maximal S_0* concentration of about 30% can be achieved with about 40% of the centers remaining in S_1 and the other 30% reacting into the S_{-1} state (*30*). As the S_1 and S_{-1} states are EPR silent under our conditions (see above), any new manganese EPR signal arising under these conditions is likely to come from S_0*. Figure 3A was obtained from an extensively dark-adapted control sample. Dark incubation on ice with hydroxylamine at a ratio of about 1 NH_2OH per 1 PS II reaction center within the EPR tube does not lead to any change in the EPR spectrum (Figure 3B). No Mn^{2+} six line signal is observed, because 1 mM EDTA was added to complex the Mn^{2+} ions. Comparative measurements without EDTA also show no multiline signal, but a Mn^{2+} signal that corresponds to about 1% of the total manganese that can be released by heat treatment (data not shown). No DCMU

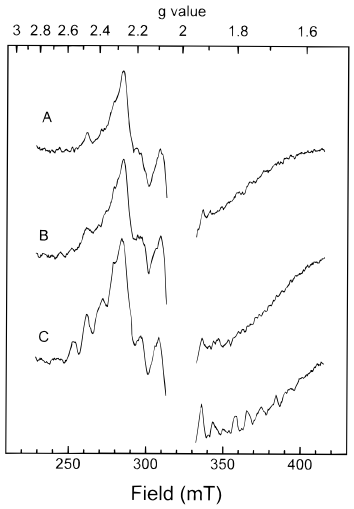

FIGURE 3: EPR spectra of dark-adapted PS II membranes ([Chl] = 14 mg/mL): spectrum A, control in the presence of 1.5% methanol and 1 mM EDTA; spectrum B, after 10 min dark incubation with 50 μM NH_2OH on ice in the EPR tube; spectrum C, was obtained after 30 s annealing of sample B at 20 °C, addition of 1.5% methanol (final concentration), further 30 s incubation at 20 °C and refreezing in liquid nitrogen. The mannitol buffer contained 1 mM EDTA for these experiments. Instrument conditions: as in Figure 1 but with temperature of 6.3 K; microwave frequency, 9.055 GHz. All spectra are the average of four scans.

and therefore no methanol was present in this sample. The sample was therefore thawed for 30 s in the dark in a water bath and then methanol was added to give a final concentration of 1.5%. The sample was then incubated at 20 °C for another 30 s and refrozen in liquid N_2. The whole treatment was completed within 2 min. The resulting spectrum is shown in Figure 3C and reveals the presence of a multiline signal. The same result was also achieved by adding the methanol before or during the initial hydroxylamine incubation. Higher methanol concentrations did not further increase the signal size, and the addition of 5% ethanol instead of methanol did not lead to the appearance of the new multiline signal (data not shown). In analogy to the situation of the S_2 state, one might expect to see a signal around $g = 4$ for the S_0* state in the absence of methanol. However, so far, we have not been able to detect such a signal in the difference spectra (data not shown). A subsequent 200 K illumination of the S_0* sample and of the control showed that the size of the S_2 multiline that could be obtained in the hydroxylamine treated sample was 42% of that induced in the control (data not shown). On the basis of previous results from the oxygen oscillation pattern, the S_0* and S_{-1} state concentrations can therefore be expected to be about 30% each (*30*).

Figure 4 compares the spectra of the S_2 state multiline signal (trace A) with three multiline signals (B, C, and D) obtained in this study under different conditions. Spectra A and D were obtained by 273 K illumination in the presence of DCMU and methanol from S_1 and S_{-1} (hydrazine) samples, respectively (the dotted middle part of D indicates, as no EDTA was added, that in this region small subtraction artifacts could be present). Spectrum B was also obtained in mannitol buffer by incubation of a long term dark-adapted sample with hydroxylamine in the presence of methanol and EDTA. The spectrum of the S_1 control sample was subtracted. Spectrum C was obtained in the same way as spectrum B, but in a buffer containing 30% ethylene glycol, 15 mM NaCl, and 20 mM Mes/NaOH, pH 6.3. A compari-

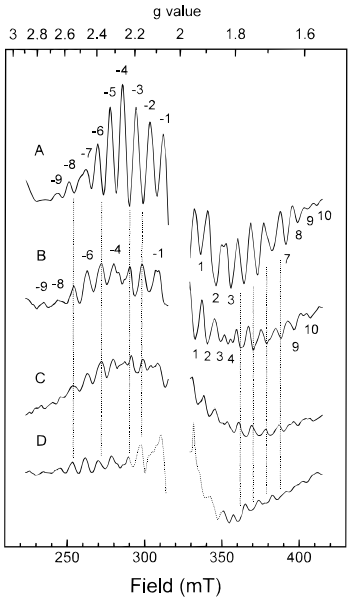

FIGURE 4: Comparison of difference EPR spectra from samples in the S_2 state (spectrum A) and in the S_0* state (spectra B, C, and D): spectrum A, light − dark difference spectrum of a sample in the S_2 state generated by 273 K illumination in the presence of 250 μM DCMU and 1.5% methanol; temperature, 8 K; microwave power, 20 mW; [Chl] = 10 mg/mL; spectrum B, S_0* multiline of a NH_2OH incubated sample minus the untreated control (S_1) in the presence of 1 mM EDTA and 1.5% methanol; temperature, 8 K, microwave power, 20 mW; [Chl] = 10 mg/mL; spectrum C, as in spectrum B, but in a buffer containing 30% ethylene glycol, 15 mM NaCl, 20 mM Mes, pH 6.3, 1 mM EDTA, 1.5% methanol; temperature, 7 K; microwave power, 30 mW; [Chl] = 14 mg/mL; spectrum D, as in Figure 2C, S_0* produced by hydrazine incubation and 273 K/DCMU illumination; no EDTA; 0.5% methanol; temperature, 6.7 K; microwave power, 10 mW; [Chl] = 20−25 mg/mL. The dotted middle part of spectrum D indicates that in this region small subtraction artifacts could be present. Instrument conditions: microwave frequency, 9.055 GHz (except trace D where it is 9.066 GHz); magnetic field modulation amplitude, 2 mT; time constant 0.3 s; scan time, 2 or 4 min. All difference spectra are the average of eight scans.

son of the four spectra reveals that (a) multiline signals B−D are very similar regardless of the presence of (e.g.) cryoprotectant, EDTA, or $CaCl_2$, and (b) the new multiline signal is distinctively different from the S_2 state multiline. These differences have been emphasized by the dotted lines which mark field positions, where the amplitudes of the new multiline signal are maximal and those of the S_2 multiline are minimal. On the basis of this overall similarity of spectra B−D, we conclude that they all originate from the S_0* state. A closer comparison of the S_0* state multilines does show that there are some differences in the peak positions on the high-field side (e.g., peaks 5, 6, 7, 8; dotted lines) especially comparing signals B and C. This is perhaps not unexpected, as it is known that the hyperfine splitting of the S_2 state multiline depends on the buffer composition.

As suggested for the S_2 multiline (*33*), the S_0* multiline seems to have a broad underlying signal. Both multilines showed similar temperature dependence and were difficult to saturate under the experimental conditions (6.7 K). $P_{1/2}$ values greater than 100 mW were measured (data not shown). The average hyperfine splittings are very similar with 8.45 mT for the S_2 state and 8.42 mT for the S_0* state multiline. However, comparing the hyperfine splittings of the low-field or the high-field parts gives slightly different results: 8.83 mT (peaks 1−8, S_2) and 7.77 mT (peaks 2−9, S_0*) for the high-field side and 8.24 (peaks −1 to −9, S_2) and 9.07 mT (peaks −1 to −9, S_0*) for the low-field side. This suggests greater anisotropy for the S_0* multiline.

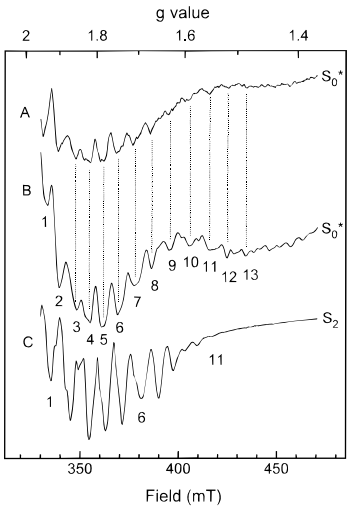

FIGURE 5: EPR spectra of the high field side of the S_0* state multiline (spectra A and B) and the S_2 state multiline (spectrum C) obtained at 6.5 K (spectra A, and C) or 4.0 K (spectrum B). Samples A and B were prepared independently by incubation with 50 μM hydroxylamine in the presents of 1 mM EDTA and 1.5% methanol for 10 min on ice ([Chl] = 14 mg/mL). Instrument conditions: spectrum A, average of 16 scans; magnetic field modulation amplitude, 1.6 mT; time constant, 0.1 s; gain, 500; microwave power, 50 mW; spectrum B, average of eight scans; magnetic field modulation amplitude, 2 mT; time constant, 0.3 s; gain 500, microwave power 30 mW; spectrum C, average of four scans; magnetic field modulation amplitude, 1.6 mT; time constant, 0.1 s; gain, 100; microwave power, 50 mW. Other conditions: scan time, 2 min; microwave frequency, 9.055 GHz.

To compare the spectral breadth of the two multiline signals we looked in detail at their high field edges (Figure 5). The high-field side was chosen because of interference by the cytb_{559} signals on the low field side. Spectra A and B were obtained at 6.5 and 4.0 K, respectively, from two separate samples enriched in the S_0* state by hydroxylamine incubation. Spectrum C was obtained at 6.5 K from a sample in the S_2 state induced by 200 K illumination. In agreement with the literature, a maximum of 10 or 11 peaks are observed for the S_2 multiline on the high-field side giving a total spectral breadth of about 180−200 mT. In contrast, in both S_0* traces, signals outside this region are clearly visible up to at least peak 13. These weak outer peaks were reproduced in at least four samples. The spectral breadth of the S_0* multiline is therefore significantly greater (at least 240 mT) than that of the S_2 state multiline. Assuming an equal number of peaks on both sides, the total number of peaks of the S_0* EPR signal is about 26, but further detailed measurements are needed to establish the exact number. This greater number of lines may in part explain the small overall amplitude of the S_0* state multiline compared to the S_2 multiline.

DISCUSSION

The data presented in this study clearly show that we have observed a new EPR multiline signal that is correlated with the S_0* state. A modified S_2 state can be ruled out as a possible origin of the signal. In the following two points will be discussed: (a) the methanol effect on the S_0* state and (b) the possible manganese oxidation states of the S_0* state.

(a) Methanol Effect. One striking observation of this study is that methanol (0.5−1.5%) is essential to observe the S_0* state multiline EPR signal and that 5% ethanol does not have a similar effect. This feature clearly distinguishes this signal from the S_2 state multiline(s), which can be observed in the absence of methanol. For S_2, alcohol enhances the amplitude of the multiline signal, as conversion from the $g = 4.1$ signal can occur. It also slightly modifies the hyperfine splitting. It is therefore possible that a very weak multiline could be present, below our present level of detection, in the S_0* state in the absence of methanol. The methanol could then modify the interactions within the Mn cluster, modifying the EPR parameters, allowing a multiline signal to be observed. However, the modification of one or more exchange interactions within the cluster could change the spin of the ground state which in turn could mean that in the absence of methanol the S_0* state would not give a multiline signal. We suggest that addition of methanol may also be helpful in future to find an EPR signal originating from the natural S_0 state produced by illumination procedures in the absence of exogenous reductants. To account for the high specificity of the methanol effect, one might speculate that the smaller methanol molecule can bind directly to the manganese cluster, while ethanol might be excluded.

(b) Possible Manganese Oxidation States in the S_0 State.* The finding of a multiline signal for the S_0* state clearly shows that the Mn ions are in a mixed valence state giving rise to a probable net spin of $S = {}^1/_2$. On the basis of the most likely Mn redox states of the S_1 and S_2 states (*1*−*5*, *17*) the following possibilities arise for the S_0* state: (a) $Mn^{II}Mn^{III}Mn^{III}Mn^{III}$, (b) $Mn^{II}Mn^{III}Mn^{IV}Mn^{IV}$, (c) $Mn^{III}Mn^{III}$-$Mn^{III}Mn^{IV}$. It was recently shown for Mn model complexes (*34*) and also in the Mn catalase (*35*, *36*) that $Mn^{II}Mn^{III}$ dimers have a greater spectral breadth than $Mn^{III}Mn^{IV}$ dimers. On the basis of these results, possibilities a and b seem to be more likely than option c. Further measurements at different microwave frequencies (Q-band and S-band) and careful simulations will hopefully result in a firmer assignment in the future.

ACKNOWLEDGMENT

The authors would like to thank P. Smith for critical reading of the manuscript. J.M. would also like to thank all those who helped him during earlier attempts to find new EPR signals in hydrazine and hydroxylamine treated samples.

REFERENCES

1. Debus, R. J. (1992) *Biochim. Biophys. Acta 1102*, 269.
2. Hansson, Ö., and Wydrzynski, T. (1990) *Photosynth. Res. 23*, 131.
3. Renger, G. (1993) *Photosynth. Res. 38*, 229.
4. Nugent, J. H. A. (1996) *Eur. J. Biochem. 237*, 519.
5. Britt, R. D. (1996) in *Oxygenic Photosynthesis: The Light Reactions* (Ort, D. R., and Yocum, C. F., Eds.), pp 137, Kluwer Academic Dordrecht.
6. Kok, B., Forbush, B., and McGloin, M. (1970) *Photochem. Photobiol. 11*, 457.
7. Vermaas, W. F. J., Renger, G., and Dohnt, G. (1984) *Biochim. Biophys. Acta 764*, 194.
8. Styring, S., and Rutherford, A. W. (1987) *Biochemistry 26*, 2401.
9. Klein, M. P., Sauer, K., and Yachandra, V. K. (1993) *Photosynth. Res. 38*, 265.
10. Dismukes, G. C., and Siderer, Y. (1981) *Proc. Natl. Acad. Sci. U.S.A. 78*, 274.
11. Åhrling, K., and Pace, R. J. (1995) *Biophys. J. 68*, 2081.
12. Bonvoisin, J., Blondin, G., Girerd, J.-J., and Zimmermann, J.-L. (1992) *Biophys. J. 61*, 1076.
13. Zheng, M., and Dismukes, G. C. (1996) *Inorg. Chem. 35*, 3307.
14. Kusunoki, M. (1992) *Chem. Phys. Lett. 197*, 108.
15. Boussac, A., Girerd, J.-J., and Rutherford, A. W. (1996) *Biochemistry 35*, 6984.
16. Smith, P. J., and Pace, R. J. (1996) *Biochim. Biophys. Acta 764*, 194.
17. Roelofs, T. A., Liang, W., Latimer, M. J., Cinco, R. M., Rompel, A., Andrews, J. C., Sauer, K., Yachandra, V. K., and Klein, M. P. (1996) *Proc. Natl. Acad. Sci. U.S.A. 93*, 3335.
18. Styring, S., and Rutherford, A. W. (1988) *Biochemistry 27*, 4915.
19. Evelo, R. G., Styring, S., Rutherford, A. W., and Hoff, A. J. (1989) *Biochim. Biophys. Acta 973*, 428.
20. Witt, H. T. (1996) *Ber. Bunsen-Ges. Phys. Chem. 100*, 1923.
21. Zimmermann, J. L., and Rutherford, A. W. (1984) *Biochim. Biophys. Acta 767*, 160.
22. Beck, W. F., and Brudvig, G. W. (1988) *J. Am. Chem. Soc. 110*, 1523.
23. Sivaraja, M., and Dismukes, G. C. (1988) *Biochemistry 27*, 6297.
24. Guiles, R. D., Yachandra, V. K., McDermott, A. E., Cole, J. L., Dexheimer, S. L., Britt, R. D., Sauer, K., and Klein, M. P. (1990) *Biochemistry 29*, 486.
25. Saygin, Ö., and Witt, H. T. (1985) *Photobiochem. Photobiophys. 10*, 71.
26. Beck, W. F., and Brudvig, G. W. (1987) *Biochemistry 26*, 8285.
27. Messinger, J., and Renger, G, (1993) *Biochemisry 32*, 9379.
28. Riggs-Gelasco, P. J., Mei, R., Yocum, C. F., and Penner-Hahn, J. E. (1996) *J. Am. Chem. Soc. 118*, 2387.
29. Messinger, J., Seaton, G., Wydrzynski, T., Wacker, U., and Renger, G. (1997) *Biochemistry 36*, 6862.
30. Messinger, J., Wacker, U., and Renger, G. (1991) *Biochemistry 30*, 7852.
31. Berthold, D. A., Babcock, G. T., and Yocum, C. F. (1981) *FEBS Lett. 134*, 231.
32. Porra, R. J., Thompson, W. A., and Kriedemann, P. E. (1989) *Biochim. Biophys. Acta 975*, 384.
33. Pace, R. J., Smith, P., Bramley, R., and Stehlik, D (1991) *Biochim. Biophys. Acta 1058*, 161.
34. Dismukes, G. C., Sheats, J. E., and Smegal, J. A. (1987) *J. Am. Chem. Soc. 109*, 7202.
35. Khangulov, S. V., Barynin, V. V., Voevodskaya, N. V., and Grebenko, A. I. (1990) *Biochim. Biophys. Acta 1020*, 305.
36. Zheng, M., Khangulov, S. V., Dismukes, G. C., and Baryin, V. V. (1994) *Inorg. Chem. 33*, 382.

BI9711285